

Retro-Leapfrog and Related Retro Map Operations

Aniela E. Vizitiu,[†] Mircea V. Diudea,^{*,†} Sonja Nikolić,[‡] and Dušanka Janežič[§]

Faculty of Chemistry and Chemical Engineering, Babes–Bolyai University, 400028 Cluj, Romania, The R. Bošković Institute, POB 180, HR-10002 Zagreb, Croatia, and National Institute of Chemistry, Hajdrihova 19, SI-1000 Ljubljana, Slovenia

Received May 11, 2006

Operations on maps are well-known theoretical tools for transforming a given polyhedral tessellation. Several theoretical investigations of fullerenes, such as their π -electronic structure and stability, need information on the original map which was transformed into a larger molecular structure. In this respect, retro-operations, particularly those of the most used leapfrog, chamfering, and capra operations, appear particularly useful in searching the associate graphs of fullerenes. A series of analyzed cages proved to be leapfrog transforms of smaller cages. This information was useful in understanding their closed π -electronic structure and related properties including the local aromaticity. An index based on the optimized geometries enabled the evaluation of aromaticity of their various substructures. Pictorial images of the π -electron distribution as the main Kekulé valence structures have been performed by the aid of the JSCHEM software package.

INTRODUCTION

Fullerenes, finite molecular cages, are currently the subject of a good deal of research and have been functionalized or inserted in supramolecular assemblies.^{1–7}

A classical fullerene is defined as a spherelike molecule, consisting entirely of carbon atoms and being tessellated by pentagons (exactly 12) and a various number of hexagons ($N/2 - 10$). Nonclassical fullerene extensions may include rings of other sizes.^{8–10}

A map M is a combinatorial representation of a closed surface.¹¹ Several transformations (i.e., operations) on maps are known and used for various purposes.

Operations on maps are topological–geometrical transformations enabling modification of a polyhedral tessellation. Basic simple map operations, such as dualization, truncation, stellation, and so forth, are well-known and have been described elsewhere.^{11–13}

Recall some basic relations in a map:¹⁴

$$\sum dv_d = 2e \quad (1)$$

$$\sum sf_s = 2e \quad (2)$$

where v is the number of vertices, e the number of edges, f the number of faces, d the vertex degree, v_d the number of vertices of degree d , and f_s the number of s -gonal faces. These two relations are combined in the famous Euler formula:¹⁵

$$v - e + f = \chi(M) = 2(1 - g) \quad (3)$$

in which χ is the Euler characteristic and g is the genus¹⁶ of a graph or the number of handles attached to the sphere to make it homeomorphic to the surface on which the given

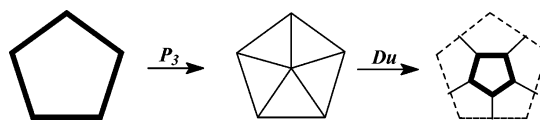


Figure 1. Leapfrog operation on a pentagonal face.

graph is embedded; $g = 0$ for a planar graph and 1 for a toroidal graph.

This paper presents three of the most commonly used map operations and their retropairs and suggests possible use of these retro-operations in investigating the π -electronic structure and stability of some fullerenes. The text is organized as follows: the next three sections present the leapfrog, quadrupling, and *capra* operations and some of the corresponding molecular realizations. The fifth section presents a case of structure investigation by the aid of retro-leapfrog. The sixth section deals with the local aromaticity evaluation, a concluding section summarizing the main results obtained.

LEAPFROG

Leapfrog (Le) is a composite operation,^{12,17–20} which can be written as

$$Le(M) = Du[P_3(M)] = Tr[Du(M)] \quad (4)$$

A sequence of stellation–dualization P_3 – Du rotates the parent s -gonal faces by π/s . Leapfrog operation is illustrated, for a pentagonal face, in Figure 1.

If M is a regular graph, the map-transformed parameters [denoted by a prime ($'$)] are

$$Le(M): v' = sf = dv; \quad e' = 3e; \quad f' = v + f \quad (5)$$

The retro-leapfrog operation is based on the following sequence:

$$RLe(M) = RP_3\{Du[Le(M)]\} \quad (6)$$

and is performed by cutting all vertices in the dual (of

* Corresponding author e-mail: diudea@chem.ubbcluj.ro.

[†] Babes–Bolyai University.

[‡] The R. Bošković Institute.

[§] National Institute of Chemistry, Slovenia

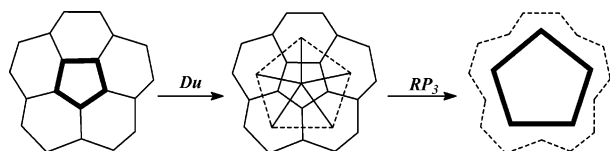


Figure 2. Retro-leapfrog operation on a pentagonal face.

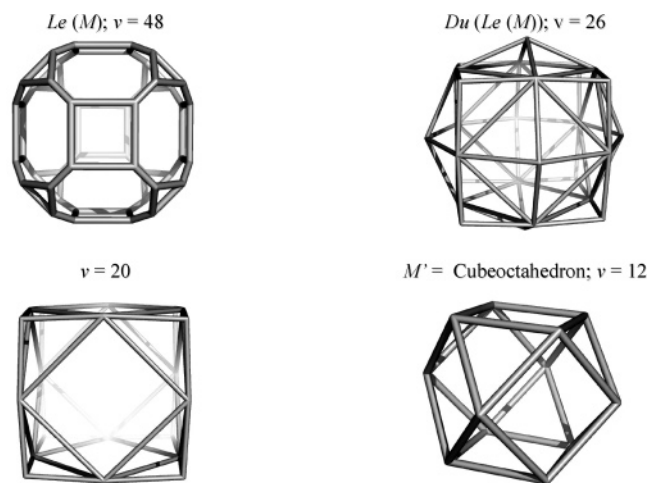


Figure 3. Retro-leapfrog operation.

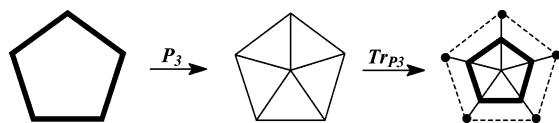


Figure 4. Quadrupling operation on a pentagonal face.

leapfrogged map) with a degree lower than the maximal one (Figure 2). Hereafter, a corresponding retro-operation is denoted by the prefix “R”. In a 3D representation, *RLe* is illustrated in Figure 3.

QUADRUPLING

Quadrupling (*Q*) is another composite operation, achieved by the sequence¹²

$$Q(M) = RE\{Tr_{P_3}[P_3(M)]\} \quad (7)$$

where *RE* denotes the (old) edge deletion (dashed lines in Figure 4) in the truncation *Tr*_{*P*₃} of each central vertex of *P*₃ capping.

The complete transformed parameters are

$$Q(M): v' = (d + 1)v; \quad e' = 4e; \quad f' = f + e \quad (8)$$

The *Q* operation leaves unchanged the initial orientation of the polygonal faces.

The retro-quadrupling operation is based on the sequence

$$RQ(M) = E\{RTr_{P_3}[P_3(M)]\} \quad (9)$$

and it is performed by adding new edges parallel to the boundary edges of the parent faces (Figure 5) and deletion of these faces. In a 3D representation, *RQ* is illustrated in Figure 6.

CAPRA

Capra, *Ca*, the goat, is the Romanian counterpart of the English children's game *leapfrog*. It is a composite opera-

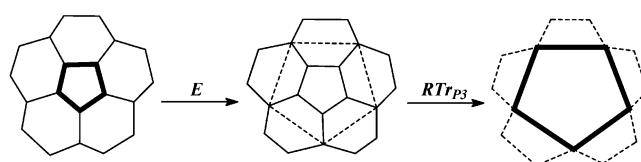


Figure 5. Retro-quadrupling operation on a pentagonal face.

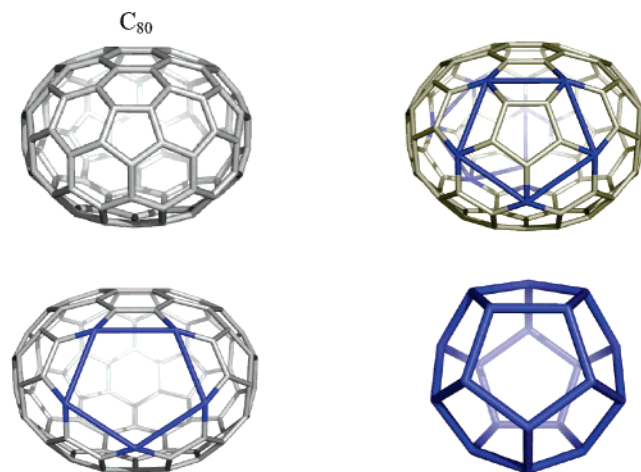
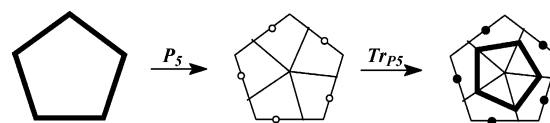


Figure 6. Retro-quadrupling operation.

Figure 7. Capra *Ca* operation on a pentagonal face.

tion,^{13,21,22} necessarily coming from Goldberg's²³ multiplying factor *m*:

$$m = (a^2 + ab + b^2); \quad a \geq b; \quad a + b > 0 \quad (10)$$

that predicts *m* (in a three-valent map) as follows: *Le*, (1, 1), *m* = 3; *Q*, (2, 0), *m* = 4; *Ca*, (2, 1), *m* = 7. In this reasoning, *Le* is also called *tripling* and *Ca* *septupling*. *Q* has also been called *chamfering*.²³

Capra is achieved by truncating *Tr*_{*P*₅}, the central vertex introduced in each of the parent faces, by a *pentangulation* *P*₅ operation (Figure 7). Note that *P*₅ involves an *E*₂ (i.e., edge trisection). This operation results in a map that preserves the original vertices while the parent *s*-gonal faces are twisted by $\pi/(3/2)s$.

The transformation can be written as

$$Ca(M) = Tr_{P_5}[P_5(M)] \quad (11)$$

Ca insulates any face of *M* by its own hexagons, which, in contrast to *Le* or *Q*, are not shared with any old face.

The complete *Ca*-transformed parameters are

$$Ca(M): v' + 2e + 2e + sf = (2d + 1)v; \quad e' = 7e; \quad f' = sf + f \quad (12)$$

The retro-capra operation is achieved by the sequence

$$RCa(M) = RE_2[RTr_{P_5}(M)] \quad (13)$$

This amounts to deleting the smallest faces of the actual map and continuing with *RE*₂ (Figure 8).

In a 3D representation, *RCa* is illustrated in Figure 9.

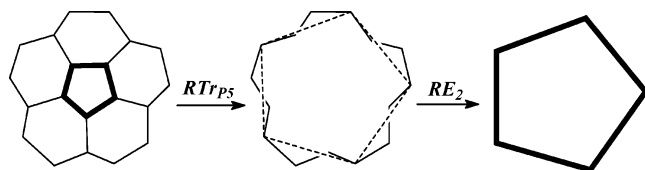


Figure 8. Retro-Capra RCa operation on a pentagonal face.



Figure 9. Retro-capra operation.



Figure 10. Two-factor structure of C_{104} ; the π -electron empty faces.

Denote a fullerene by F and its retro operation by $R\Omega(F) = F'$. At the question “does such an F' cage exist?” the answer is no, if the retro-operation will produce an irregular graph, eventually having dangling bonds; otherwise, the answer is yes. Some other data, such as those derived from eqs 5, 8, and 12, can also shed some light on this question.

If F' cannot exist, no specific properties, derived from the above operations (see the next section), can be assigned to F . Consider, for example, the fullerenes C_{80} , 80:1; D_{5d} and 80:6; D_{5h} , from the Atlas of Fullerenes.²⁴ The first one is the quadrupling of C_{20} , but the other is not. The molecule with D_{5d} symmetry will preserve the character of the orbitals in C_{20} [the degeneracy of the highest occupied molecular orbital (HOMO) and the lowest unoccupied molecular orbitals, LUMO, LUMO+1, and LUMO+2], which is not the case for the molecule with D_{5h} symmetry. The three operations discussed above preserve, at least in part, the symmetry of the parent structures, so that the knowledge of the operation involved in the construction of a fullerene is useful in structure elucidation studies.²⁵

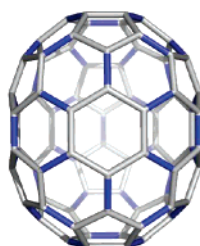
STRUCTURE INVESTIGATION BY RETRO-LEAPFROG

The properly closed-shell fz-tubulenes²⁶ (i.e., cages having fullerene halves as caps for a “zigzag” tube) obey a true leapfrog rule, written for zigzag cylinders, Z-LER: $N = 13k + 3km$; $k = 4, 6, 8, \dots$; $m = 1, 2, \dots$ Indeed, such objects show a two-factor (i.e., a disjoint set of faces, built up on all vertices in M —Figure 10)^{26,27} and also defined radialene substructures (Figure 11). A two-factor, sometimes called a perfect Clar structure,²⁷ is associated with a Fries structure,²⁸ which is a Kekulé structure having the maximum possible number of benzenoid (alternating single–double edge) faces.

Such structures represent fully resonant molecules^{29,30} and are expected to be extremely stable, in terms of the valence bond theory.^{27,29,30}

The closed-shell π -electronic structure of these cages is reflected in the HOMO–LUMO gap, in both the simple

(a) C_{78} ; $k=6$; side



(b) C_{78} ; $k=6$; top

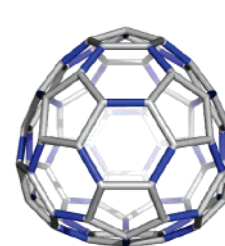


Figure 11. Kekulé valence structure; (a) coronene substructure of radialenic type $(0,3^6)$; (b) triphenylenic substructure $(3(0,3)^3)$.

C_{26} ; $\text{deg}=3$; side



C_{26} ; $\text{deg}=3$; top



C_{34} ; $\text{deg}=4$; side



C_{34} ; $\text{deg}=4$; top

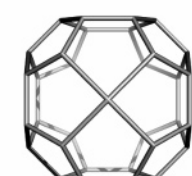


Figure 12. Parent small cages of C_{78} and C_{104} , respectively, obtained by RLe .

Hückel level of theory and PM3 calculations (Table 1). The heat of formation HF values of the cages with the polar ring between $k = 6$ and 10 are low. The PM3 energy for C_{60} is about 13.5 kcal/mol.

Although some exceptions have been observed,²⁴ a closed structure of the π -electronic shell was found²⁵ to be a general property of cages derived by the Le operation performed on smaller cubic/trivalent cages. The cages in Table 1 all represent properly closed-shell molecules, despite the fact that the parent small cages (derived by the retro RLe operation—Figure 12) have nontrivalent atoms in the polar rings.

A previous paper³¹ contained an erroneous assessment of the Z-LER rule as a distinct zigzag rule, ZCR. This was due to the absence of an immediate relationship with the leapfrog operation for the cages having $k \neq 6$.

The LUMO orbital is a non-bonding orbital in the case of $0[\text{mod}(k,4)]$ cages, Table 1, entries 1 and 3. Notably, the cap $C_{13k/2k(56)^{k/2}(665)^{k/2}-Z[3k,0]}$, $k = 6$, is C_{60} -deducible, if a hexagon is taken as the polar ring. The subscript derives from the spiral code.^{24,26,32}

The strain energy SE, in terms of POAV1 theory,^{33–36} decreases as the cage size increases (Table 2). For comparison, SE for C_{60} is about 8.26 kcal/mol.

LOCAL AROMATICITY

The aromaticity of totally resonant benzenoid molecules was discussed in detail by Randić in a recent review.³⁰ A geometric criterion of aromaticity, the index called HOMA (harmonic oscillator model of aromaticity)^{37–40} was derived from the difference between the actual and the average CC

Table 1. Data for fz-Tubulenes $C_{N\{k(56)^{k/2}(665)^{k/2}-Z[3k,0]\}}$

	cage k	N	symmetry	PM3	PM3 gap (eV)	Hückel data			
				HF/at. (kcal/mol)		HOMO	LUMO	gap ($ \beta $ units)	shell
1	4	52	D_{2h}	21.585	5.533	0.256	0	0.256	properly closed
2	6	78	C_{3h}	12.294	6.083	0.516	-0.118	0.633	properly closed
3	8	104	C_{4h}	11.453	5.730	0.256	0	0.256	properly closed
4	10	130	C_{5h}	12.518	5.998	0.458	-0.087	0.545	properly closed

Table 2. Data for fz-Tubulenes $C_{N\{k(56)^{k/2}(665)^{k/2}-Z[3k,0]\}}$

	cage k	SE(POAV1) (kcal/mol)	HOMA (global)	[6]Cor(6) (0,3 ⁶)	[5]Cor(6) (0,3 ⁵)	[k]Cor(5,6) [($k/2$)(0,3) ^{$k/2$}]	triphenylene ^a
	1	2	3	4	5	6	7
1	4	12.526	-0.096	0.060	0.188	-0.364	0.093 (0,3) ^c 0.133 (3,3) ⁿ 0.224 (3,2,3) ^{pc}
2	6	6.794	0.231	0.327	0.291 ^{pc} 0.292	0.184	0.258 (3,3) ^p 0.320 (3,3) ^{pc} 0.333 (0,3) ^c 0.350 (3,3) ⁿ
3	8	5.218	0.177	0.425	0.347	0.042	0.380 (3,3) ^{pc} 0.428 (3,3) ⁿ 0.433 (0,3) ^c
4	10	4.999	-0.164	0.517	0.338	-0.770	0.353 (3,3) ^{pc} 0.511 (3,3) ⁿ 0.542 (0,3) ^c

^a n indicates the normal triphenylene, c the coronene unit, and p and pc stand for the “polar” and “polar-circle” regions, respectively.

bond lengths. The HOMA index can be used to search the local aromaticity of various substructures. The data in Table 2 are calculated as in ref 40.

The coronene [6]Cor(6) substructure is of radialenic type (0,3⁶) in these cages, as appears in the main Kekulé valence structure; no alternating (3(0,3)³) covering was observed. The numbers in parentheses in Table 2 represent the numeric Kekulé structures, as proposed by Randić.⁴¹ Their HOMA values increase as the cage size increases (Table 2, column 4), and the same is true for the [5]Cor(6) substructure (Table 2, column 5), which is also radialenic (0,3⁵).

The flower⁴² at the pole, the corannulenic substructure, with alternating (5,6) faces around the core (Table 2, column 6) shows the covering (($k/2$)(0,3) ^{$k/2$}), except when $k = 4$, for which a (($k/2$)(1,2) ^{$k/2$}) covering was observed, with corresponding modification of the neighbor [5]Cor(6) to (0,2,3⁴). Their HOMA values are representative of the global aromaticity, as shown in Table 2, column 3. Clearly, the most aromatic structure is the cage with $k = 6$, corresponding to the isolated C₇₈ fullerene.

It is remarkable that, for the cage with $k = 8$, both the heat of formation HF (Table 1, row 3) and strain energy SE (in POAV1 terms, Table 2, row 3, column 2) data show lower values than those for the cage with $k = 6$, suggesting a higher stability for the former. However, the HOMO–LUMO gap for the cage with $k = 8$ is lower than that for the cage with $k = 6$, both at the Hückel and the PM3 level of theory (Table 1), indicating a kinetic instability, which is additionally supported by the nonbonding character of the LUMO orbital, in Hückel theory.

Triphenylenic substructures show the covering (3,3³) [(0,3³) for the substructure included in the coronene units—Table 2, column 7] in the main Kekulé valence structure. Even the coronene [6]Cor(6) substructure shows no alternating (3(0,3)³) covering; the HOMA values for the included triphenylenic units are higher than those for the normal, fully

populated (3,3³) triphenylenic units, in cages with $k = 8$ and 10 (Table 2, rows 3 and 4, column 7). This is due to the increased HOMA values for coronene units, at the expense of the remaining substructures of these cages. The cage with $k = 6$, representing the isolated C₇₈ fullerene, a fully benzenoid, 6n π -electron structure,³⁰ shows a more uniform repartition of the local aromatic character, and this is probably the most important reason for its stability. Thus, the true ordering of aromaticity for triphenylenic units, according to the π -electron population as given by the numeric Kekulé structures, is that of the cage with $k = 6$ (Table 2, row 2, column 7). Note the importance of the level of theory according to the optimization of molecules that is made. The most accurate results are reported in the case of bond lengths calculated by an ab initio approach or, better, derived from experimental data, such as X-ray diffraction and neutron diffraction.⁴⁰

In the above discussion, the main Kekulé valence structure is that drawn, on the PM3 optimized cage, by the software program JSCHM,⁴³ with an appropriate separation threshold between single and double bonds. Taken from thousands of geometric Kekulé valence structures, the C₇₈ cage (Figure 11), 78:4, in the atlas of fullerenes,²⁴ with a Kekulé structure count $K = 195\,952$,⁴⁴ can be viewed as an “experimental” structure, it giving a pictorial image of the π -electron distribution. This main Kekulé valence structure shows the maximal number of Kekulé benzene rings and accordingly is identified with the Fries²⁸ valence structure, or a Clar^{45,46} structure, which is a valence structure with the maximal number of disjointed aromatic π sextets, and it is the result of the superposition of all geometric Kekulé structures with the highest degree of freedom.³⁰

Returning to the notion of two-factor, discussed above, a perfect Clar structure, PCS, refers precisely to the two-factor, not to the Clar structure, as generally accepted.^{45,46} Here, the cycles forming a PCS are empty (not populated with π

electrons), at least in some of the Kekulé valence structures. Only in all-polyhex systems, like polyhex toroids, where it is possible to change the assessment full/empty, at two neighboring hexagons, may the PC rings be full of π electrons, thus following the original idea of Clar. In this view, an “empty” octagon can exist in a fully conjugated aromatic system (see also refs 27 and 42).

CONCLUSIONS

Operations on maps and their retro-transformations, particularly those of the most used operations leapfrog, chamfering, and capra, have proved to be useful in investigating the properties of fullerenes, particularly their π -electronic structure and stability. Such operations preserve, at least in part, the symmetry of the parent cages, which is important in establishing relationships among fullerenes. Thus, a series of Z-LER cages proved to be leapfrog transforms of smaller cages. This information was useful in understanding their closed π -electronic structure and related properties including the local aromaticity. The HOMA index enabled the evaluation of aromaticity of their various substructures.

This led to an understanding of the stability of the cage with $k = 6$, representing the isolated C_{78} fullerene, as the result of a more uniform repartition of the aromaticity of their substructures. Pictorial images of the π -electron distribution as the main Kekulé valence structures have been performed with the aid of the JSCHEM software package.

ACKNOWLEDGMENT

The authors are grateful to the reviewers for their useful comments. A financial support from the Billateral Romania-Slovenia Project is also acknowledged.

REFERENCES AND NOTES

- (1) Taylor, R. *The Chemistry of Fullerenes*; World Scientific: Singapore, 1995.
- (2) Dresselhaus, M. S.; Dresselhaus, G.; Eklund, P. C. *Science of Fullerenes and Carbon Nanotubes*; Academic Press: San Diego, CA, 1996.
- (3) Neretin, I. S.; Lyssenko, K. A.; Antipin, M. Yu.; Slovokhotov, Yu. L.; Boltalina, O. V.; Troshin, P. A.; Lukonin, A. Yu.; Sidorov, L. N.; Taylor, R. $C_{60}F_{18}$, a Flattened Fullerene: Alias a Hexa-Substituted Benzene. *Angew. Chem., Int. Ed.* **2000**, *39*, 3273–3276.
- (4) Qian, W.; Rubin, Y. A Parallel Library of All Seven $A_2+B_2+C_2+T_h$ Regioisomeric Hexakisadducts of Fullerene C_{60} : Inspiration from Werners' Octahedral Stereoisomerism. *Angew. Chem., Int. Ed.* **2000**, *39*, 3133–3137.
- (5) Lee, K.; Lee, Ch. H.; Song, H.; Park, J. T.; Chang, H. Y.; Choi, M.-G. Interconversion between μ - η^2 , η^2 - C_{60} and μ_3 - η^2 , η^2 - C_{60} on a Carbido Pentaosmium Cluster Framework. *Angew. Chem., Int. Ed.* **2000**, *39*, 1801–1804.
- (6) Fässler, T. F.; Hoffmann, R.; Hoffmann, S.; Wörle, M. Triple-Decker Type Coordinations of a Fullerene Trianion in $[K([18]Crown-6)]_3-[\eta^6-C_{60}](\eta^3-C_6H_5-CH_3)_2$ -Single Crystal Structure and Magnetic Properties. *Angew. Chem., Int. Ed.* **2000**, *39*, 2091–2094.
- (7) Wang, G. W.; Zhang, T. H.; Hao, E. H.; Jiao, L. J.; Murata, Y.; Komatsu, K. Solvent-Free Reactions of Fullerenes and N-Alkylglycines with and without Aldehydes under High-Speed Vibration Milling. *Tetrahedron* **2003**, *59*, 55–60.
- (8) Mackay, A. L.; Terrones, H. Diamond from Graphite. *Nature* **1991**, *352*, 762–762.
- (9) Gao, Y.-D.; Herndon, W. C. Fullerenes with Four-Membered Rings. *J. Am. Chem. Soc.* **1993**, *115*, 8459–8460.
- (10) Fowler, P. W.; Heine, T.; Manolopoulos, D. E.; Mitchell, D.; Orlandini, G.; Schmidt, R.; Seifert, G.; Zerbetto, F. Energetics of Fullerenes with Four-Membered Rings. *J. Phys. Chem.* **1996**, *100*, 6984–6991.
- (11) Pisanski, T.; Randić, M. Bridges between Geometry and Graph Theory. In *Geometry at Work: a Collection of Papers Showing Applications of Geometry*; Gorini, C. A., Ed.; Mathematical Association of America: Washington, DC, 2000; Vol. 53, pp 174–194.
- (12) Diudea, M. V.; John, P. E.; Graovac, A.; Primorac, M.; Pisanski, T. Leapfrog and Related Operations on Toroidal Fullerenes. *Croat. Chem. Acta* **2003**, *76*, 153–159.
- (13) Diudea, M. V. Covering Forms in Nanostructures. *Forma (Tokyo)* **2004**, *19*, 131–163.
- (14) Euler, L. Solutio Problematis ad Geometriam Situs Pertinentis. *Comment. Acad. Sci. I. Petropolitanae* **1736**, *8*, 128–140.
- (15) Euler, L. Elementa Doctrinae Solidorum Novi. *Comment. Acad. Sci. I. Petropolitanae* **1758**, *4*, 109–160.
- (16) Harary, F. *Graph Theory*; Addison-Wesley: Reading, MA, 1969.
- (17) Eberhard, V. *Zur Morphologie der Polyeder*; Teubner: Leipzig, 1891.
- (18) Fowler, P. W. How Unusual is C_{60} ? Magic Numbers for Carbon Clusters. *Chem. Phys. Lett.* **1986**, *131*, 444–450.
- (19) Fowler, P. W.; Steer, J. I. The Leapfrog Principle: A Rule for Electron Counts of Carbon Clusters. *J. Chem. Soc., Chem. Commun.* **1987**, 1403–1405.
- (20) Dias, J. R. From Benzenoid Hydrocarbons to Fullerene Carbons. *MATCH* **1996**, *33*, 57–85.
- (21) Diudea, M. V. Capra-A Leapfrog Related Operation on Maps. *Stud. Univ. Babeş-Bolyai, Chem.* **2003**, *48* (2), 3–16.
- (22) Diudea, M. V. Nanoporous Carbon Allotropes by Septupling Map Operations. *J. Chem. Inf. Model.* **2005**, *45*, 1002–1009.
- (23) Goldberg, M. A Class of Multi-Symmetric Polyhedra. *Tohoku Math. J.* **1937**, *43*, 104–108.
- (24) Fowler, P. W.; Manolopoulos, D. E. *An Atlas of Fullerenes*; Oxford University Press: London, 1994; pp 254–255.
- (25) King, R. B.; Diudea, M. V. The Chirality of Icosahedral Fullerenes: A Comparison of the Tripling (Leapfrog), Quadrupling (Chamfering), and Septupling (Capra) Transformations. *J. Math. Chem.* **2006**, *39*, 597–604.
- (26) Diudea, M. V. Stability of Tubulenes. *Phys. Chem. Chem. Phys.* **2004**, *6*, 332–339.
- (27) Fowler, P. W.; Pisanski, T. Leapfrog Transformations and Polyhedra of Clar Type. *J. Chem. Soc., Faraday Trans.* **1994**, *90*, 2865–2871.
- (28) Fries, K. Über Bicyclische Verbindungen und Ihren Vergleich mit dem Naphtalin. *J. Liebigs Ann. Chem.* **1927**, *454*, 121–324.
- (29) Dias, J. R. The Most Stable Class of Benzenoid Hydrocarbons and Their Topological Characteristics—Total Resonant Sextet Benzenoids Revisited. *J. Chem. Inf. Comput. Sci.* **1999**, *39*, 144–150.
- (30) Randić, M. Aromaticity of Polycyclic Conjugated Hydrocarbons. *Chem. Rev.* **2003**, *103*, 3449–3605.
- (31) Diudea, M. V. The Zig-Zag Cylinder Rule. *Stud. Univ. Babeş-Bolyai, Chem.* **2003**, *48*, 31–40.
- (32) Diudea, M. V.; Nagy, Cs. L.; Silaghi-Dumitrescu, I.; Graovac, A.; Janežič, D.; Vikić-Topić, D. Periodic Cages. *J. Chem. Inf. Model.* **2005**, *45*, 293–299.
- (33) Haddon, R. C. Rehybridization and π -Orbital Overlap in Nonplanar Conjugated Organic Molecules: π -Orbital Axis Vector (POAV) Analysis and Three-Dimensional Hückel Molecular Orbital (3D-HMO) Theory. *J. Am. Chem. Soc.* **1987**, *109*, 1676–1685.
- (34) Haddon, R. C. Measure of Nonplanarity in Conjugated Organic Molecules: Which Structurally Characterized Molecule Displays the Highest Degree of Pyramidalization? *J. Am. Chem. Soc.* **1990**, *112*, 3385–3389.
- (35) Haddon, R. C. C_{60} : Sphere or Polyhedron? *J. Am. Chem. Soc.* **1997**, *119*, 1797–1798.
- (36) Haddon, R. C.; Chow, S.-Y. Hybridization as a Metric for the Reaction Coordinate of Chemical Reactions. *J. Am. Chem. Soc.* **1998**, *120*, 10494–10496.
- (37) Julg, A.; Francois, Ph. Structural Studies of Some Non-Alternant Hydrocarbons; a New Definition of Aromaticity. *Theor. Chim. Acta* **1967**, *7*, 249–261.
- (38) Krygowski, T. M. Crystallographic Studies of Inter- and Intra-Molecular Interactions Reflected in Aromatic Character of n-Electron Systems. *J. Chem. Inf. Comput. Sci.* **1993**, *33*, 70–78.
- (39) Krygowski, T. M.; Ciesielski, A. Aromatic Character in the Benzene Ring Present in Various Topological Environments in Benzenoid Hydrocarbons. Nonequivalence of Indices of Aromaticity. *J. Chem. Inf. Comput. Sci.* **1995**, *35*, 203–210.
- (40) Krygowski, T. M.; Ciesielski, A. Local Aromatic Character of CSO and C,O and Their Derivatives. *J. Chem. Inf. Comput. Sci.* **1995**, *35*, 1001–1003.
- (41) Randić, M. Algebraic Kekulé Formulas for Benzenoid Hydrocarbons. *J. Chem. Inf. Comput. Sci.* **2004**, *44*, 365–372.
- (42) Diudea, M. V. Corannulene and Corazulene Tiling of Nanostructures. *Phys. Chem. Chem. Phys.* **2005**, *7*, 3626–3633.
- (43) Nagy, Cs. L.; Diudea, M. V. *JSCHEM Software Package*; Babeş-Bolyai University: Cluj, Romania, 2005.
- (44) Vukićević, D. Personal communication.
- (45) Clar, E. *Polycyclic Hydrocarbons*; Academic Press: London, 1964.
- (46) Clar, E. *The Aromatic Sextet*; Wiley: New York, 1972.